ARTICLE
TMR Pharmacology Research 2023;3(2):6. https://doi.org/10.53388/PR202303006

Exploring the anti-cancer effect of taraxasterol using network pharmacology, molecular docking and in vitro experimental validation

Jian-Lin Yang[1#], Yi-Han Hong[1#], Ju-Min Xie[1*], Hui Mao[2*], Shi-Nuan Fei[3*]

[#]Jian-Lin Yang and Yi-Han Hong are the co-first authors of this paper.

[1]Hubei Key Laboratory of Renal Disease Occurrence and Intervention, School of Medicine, Hubei Polytechnic University, Huangshi 435003, China. [2]Department of Dermatology, Huangshi Central Hospital, Huangshi 435000, China. [3]Department of Pediatrics, Huangshi Maternal and Child Health Care Hospital, Huangshi 435003, China.

[*]**Corresponding to:** Ju-Min Xie, Hubei Key Laboratory of Renal Disease Occurrence and Intervention, School of Medicine, Hubei Polytechnic University, No. 16, Guilin North Road, Huangshi 435003, China. E-mail: xiejumin@hbpu.edu.cn. Hui Mao, Department of Dermatology, Huangshi Central Hospital, No. 141, Tianjin Road, Huangshi 435000, China. E-mail: maohui1970@163.com. Shi-Nuan Fei, Department of Pediatrics, Huangshi Maternal and Child Health Care Hospital, No. 80, Guilin South Road, Huangshi 435003, China. E-mail: Feishinuan@163.com.

Author contributions

Ju-Min Xie, Jian-Lin Yang and Yi-Han Hong conceived this study, carried out this study, and drafted the manuscript. Ju-Min Xie designed the study, collected and analyzed the data. Hui Mao and Shi-Nuan Fei helped accomplish the conception and design of the study. Ju-Min Xie, Hui Mao and Shi-Nuan Fei were responsible for this manuscript and reviewed the article critically. All authors read and approved the final manuscript.

Competing interests

The authors declare no conflicts of interest.

Acknowledgments

This study was supported by local special projects in major health of Hubei Provincial Science and Technology Department (2022BCE054) and key scientific research projects of Hubei polytechnic University (23xjz08A).

Peer review information

TMR Pharmacology Research thanks all anonymous reviewers for their contribution to the peer review of this paper.

Abbreviations

TS, taraxasterol; PPI, protein-protein interaction; GO, gene ontology; KEGG, Kyoto Encyclopedia of Genes and Genomes; HDAC1, histone deacetylase 1; ESR1, estrogen receptor 1; AR, androgen receptor; MAPK1, mitogen-activated protein kinase 1.

Citation

Yang JL, Hong YH, Xie JM, Mao H, Fei SN. Exploring the anti-cancer effect of taraxasterol using network pharmacology, molecular docking and in vitro experimental validation. *TMR Pharmacol Res.* 2023;3(2):6. doi: 10.53388/PR202303006.

Executive editor: Shan-Shan He.

Received: 19 January 2023; **Accepted:** 23 May 2023; **Available online:** 6 June 2023.

Abstract

Taraxasterol (TS) is a naturally occurring pentacyclic triterpenoid extracted from the traditional Chinese herb *Taraxacum mongolicum*. Previous studies have highlighted its significant roles in exhibiting anti-inflammatory, anti-oxidant, and liver protective effects. In the present study, the anti-cancer potential of TS against cervical cancer was investigated, employing network pharmacology techniques, molecular docking, and in vitro experimental validation. TS exhibits its anticancer properties by modulating multiple targets, pathways, and biological processes. In vitro experiments demonstrated the potent inhibitory effects of TS on cancer cell growth and migration, while no significant impact on apoptosis was observed. The primary objective was to elucidate the anti-cancer potential of TS, which is a crucial lead compound in the treatment of cervical cancer. The findings may serve as a basis for the development of novel anticancer therapeutics and medicine-based interventions for cervical cancer.

Keywords: anti-cancer; molecular docking; network pharmacology; taraxasterol

Highlights

Taraxasterol is a naturally produced marker molecule of Taraxacum mongolicum, which contains nearly 100 ingredients and is used to treat 181 different kinds of diseases.

Taraxasterol exerts an anti-cancer effect through multiple targets, pathways, and biological processes based on network pharmacology and molecular docking validation.

In vitro experiments confirmed that taraxasterol played significant roles in inhibiting cancer cell growth, and migration but not apoptosis.

Introduction

As GLOBOCAN 2020 was released, about 19.3 million new cancer cases and 10 million cancer deaths were reported in 185 countries for the 36 documented cancers [1]. Based on the data provided by the World Health Organization, cancer is emerging as the primary cause of human fatalities worldwide, posing a significant threat to human physical well-being and escalating the financial strain of cancer management [1–3]. In addition to surgical resection, chemotherapy, radiotherapy, and immunotherapy are also gradually improving from lab research to clinical trials. The increased expenditure and economic load of cancer therapy collapsed most of the patient families in China [4, 5]. For more than 3,000 years, traditional Chinese herbs and formulas have been extensively used in China for managing various ailments. Nowadays, they are garnering increasing attention for their promising potential in treating malignancies. With the expansion of basic research, numerous traditional Chinese herbs are being explored for the extraction of unidentified bioactive compounds with potential therapeutic applications [6].

In recent times, traditional Chinese medicine has drawn considerable attention for its potential in the management of cancer. Several hundreds of Chinese herbs have emerged as research hotspots for tackling the disease. Among them, *Taraxacum mongolicum Hand Mazz*, also commonly known as dandelion, has gained significant attention in the realm of cancer treatment [7–9]. Dandelion has featured in over 100 traditional Chinese prescriptions due to its inclusion in the 2015 edition of the Chinese Pharmacopeia [10]. Dandelion is well-recognized and has been long-term used as a dietary and medicinal plant in China, where it can treat almost 181 types of disease [9, 10]. The huge medicinal functions of dandelion were based on its' constitution, including, for instance, flavonoids, sesquiterpene lactones, phenolic acids, vitamins, polysaccharides, amino acids, triterpenoids, pigments, coumarins, and sterols [11, 12]. The active compounds present in dandelion authorize its beneficial effects in anti-cancer, anti-thrombosis, anti-inflammatory, hypoglycemia, anti-oxidation, and immune regulation [9, 13–15].

Taraxasterol (TS) is a naturally occurring pentacyclic triterpenoid, and one of the active compounds that can be extracted from dandelion [10, 16]. Previous studies have affirmed the essential functions of TS in liver protection, anti-oxidation, anti-inflammatory, and various other significant pharmacological activities [17–22].

This study sought to elucidate the anti-cancer effects of TS in cervical cancer using network pharmacology, molecular docking, and in vitro experimental validation. The results highlight the significance of traditional Chinese herbs, precious active compounds, associated target genes, and novel ideas in cancer therapy.

Materials and methods

TS evaluation and targets collection

Evaluation of TS was performed through the SwissADME platform (http://www.swissadme.ch) and the Traditional Chinese Medicine Systems Pharmacology database (TCMSP, https://tcmsp-e.com/) [16, 23]. Due to Lipinski's RO5 criterion, oral bioavailability (OB) ≥ 30% (or high GI absorption), and drug-likeness (DL) ≥ 0.18 [24].

Targets were searched in the Swiss Target Prediction database (http://swisstargetprediction.ch/), and the targets were effectiveness when probability ≥ 0.1 [25]. In addition, Super-PRED (https://prediction.charite.de/) and PharmMapper (http://lilab-ecust.cn/pharmmapper/index.html) were used to fully collect the putative targets through distinct algorithms and mechanisms [26, 27].

Cancer-related targets identification

Cancer-related targets were obtained from the GeneCards database (https://www.genecards.org/), the Online Mendelian Inheritance in Man (OMIM, https://www.omim.org/) and the Therapeutic Targets Database (TTD database, http://db.idrblab.net/ttd/) [28–30]. The organism was set to "*Homo sapiens,*" and "cervical cancer" served as the keyword used to identify putative targets. Targets retrieved from GeneCards with a relevance score of 10 or greater were included in the analysis.

"TS-targets-cervical cancer" network construction

TS and cervical cancer intersected targets were obtained through Venny 2.1.0 (https://bioinfogp.cnb.csic.es/tools/venny/). The "TS-targets-cervical cancer" network was constructed and visualized through Cytoscape (version 3.8.0) software (https://cytoscape.org/) [31].

Protein-protein interaction (PPI) network construction

The STRING database (version 11.5) (https://cn.string-db.org/) was utilised to compute the PPI network for the shared targets of TS and cervical cancer [32]. The study organism was "Homo sapiens", and interactions with a minimum required score of ≥ 0.4 were deemed significant [33]. Cytoscape was employed to visualise and scrutinise the PPI network. Hub targets were selected based on previously reported criteria with node size corresponding to degree value, whereby larger nodes represent higher degree values [7, 34, 35].

Target clustering analysis

Target clustering was analyzed through the Cytoscape app plugin MCODE [36]. The criteria were referred to in our previous study [7].

Gene ontology (GO) and Kyoto Encyclopedia of Genes and Genomes (KEGG) enrichment analysis

Biological functions and pathways of targets were done through GO (http://geneontology.org/) and KEGG (https://www.genome.jp/kegg/) [37, 38]. The visualization of terms was done through the imageGP online tools (http://www.ehbio.com/ImageGP/index.php/) [39]. The KEGG enriched pathways network was constructed through Cytoscape. The balls represented the targets, and the squares were enriched KEGG pathways.

Molecular docking

Molecular docking between TS and hub targets was performed to validate interaction through Autodock Vina (https://vina.scripps.edu/) software [40, 41]. The TS-hub target association was visualized using PyMoL (version 2.2) (http://www.pymol.org/2/). All the performance details and parameters set were refered to in our previous report [7]. The 2D molecular docking interaction was conducted through the ProteinsPlus web service (https://proteins.plus) [42]. When the affinity score was ≤ − 5.0 kcal/mol, which represents strong interactions between the core targets and TS [43].

Expression pattern and overall survival analysis

Sanger-box 3.0 website tools (http://vip.sangerbox.com/home.html) collected a unified, standardized pan-cancer data set, TCGA TARGET GTEx from UCSC (https://xenabrowser.net/) database. Cancer species with fewer than 3 samples were excluded, and finally, we obtained the

expression data in cervical squamous cell carcinoma and endocervical adenocarcinoma. Overall survival analysis was performed through GEPIA [44].

Cell culture

HeLa-S3 were purchased from ATCC and grown in Dulbecco's modified Eagle's medium containing 10% fetal bovine serum and 1% penicillin/streptomycin. The cells were routinely maintained in 5% CO_2 at 37 ˚C. The culture medium was refreshed every 48 hours. For cell passage, the cells were digested with 0.25% trypsin. When grown as an adherent monolayer with a logarithmic growth stage, the cells were used for experiments.

Cell viability assay

The MTT assay (Beyotime) was employed to analyze cell viability. HeLa-S3 cells were diluted to a density of (1×10^5/mL), and 100 μL was seeded into a 96-well plate in quadruplicate. After 16 hours of incubation, TS was administered at final concentrations of 0, 0.5, 2.5, 5, 10, 15, and 20 μg/mL for 24, 48, and 72 hours, respectively. Following a 4-hour incubation with MTT reagent at 37 ˚C, formazan solution was added into the wells. Once the formazan was completely dissolved, cell viability was measured at 570 nm using a microtiter plate reader (Molecular Devices).

Cell migration assay

To investigate the effect of TS on cell migration, a wound healing assay was conducted. HeLa-S3 cells were seeded into a 6-well plate at a density of 3×10^5/mL. Once the cell confluence reached 90%, a straight scratch was made using tips. TS was administered at a final concentration of 15 μg/mL for 24, 48, and 72 hours, respectively. Subsequently, photos were captured and areas were calculated using Image J.

Colony-forming assay

A 6-well plate was utilized to seed cells at a density of 1×10^4/mL. TS was administered at a final concentration of 15 μg/mL for 7 days, with the cell culture medium being refreshed every 2 days. Colonies were fixed with 4% (wt/vol) paraformaldehyde for 30 minutes and stained with 1% crystal violet for 15 minutes. Photos were taken and analyzed with Image J. Colonies with more than 50 cells but less than 1000 cells were counted.

Results

Target genes screening

A total of 216 targets correlated with TS were achieved due to the intersection of Super-PRED, PharmMapper, and Swiss Target Prediction (Figure 1). Then, we used "cervical cancer" as the keyword to search for associated genes in the GeneCards, OMIM, and TTD databases. GeneCards obtained 1303 targets with a relevance score ≥ 10,497 in OMIM, and 14 in TTD (up to November 1, 2022). Through Venny 2.1, 1694 intersected targets correlated with cervical cancer were achieved (Figure 1). Moreover, 66 shared targets were obtained (Figure 1), and the detailed information was listed in (Table 1).

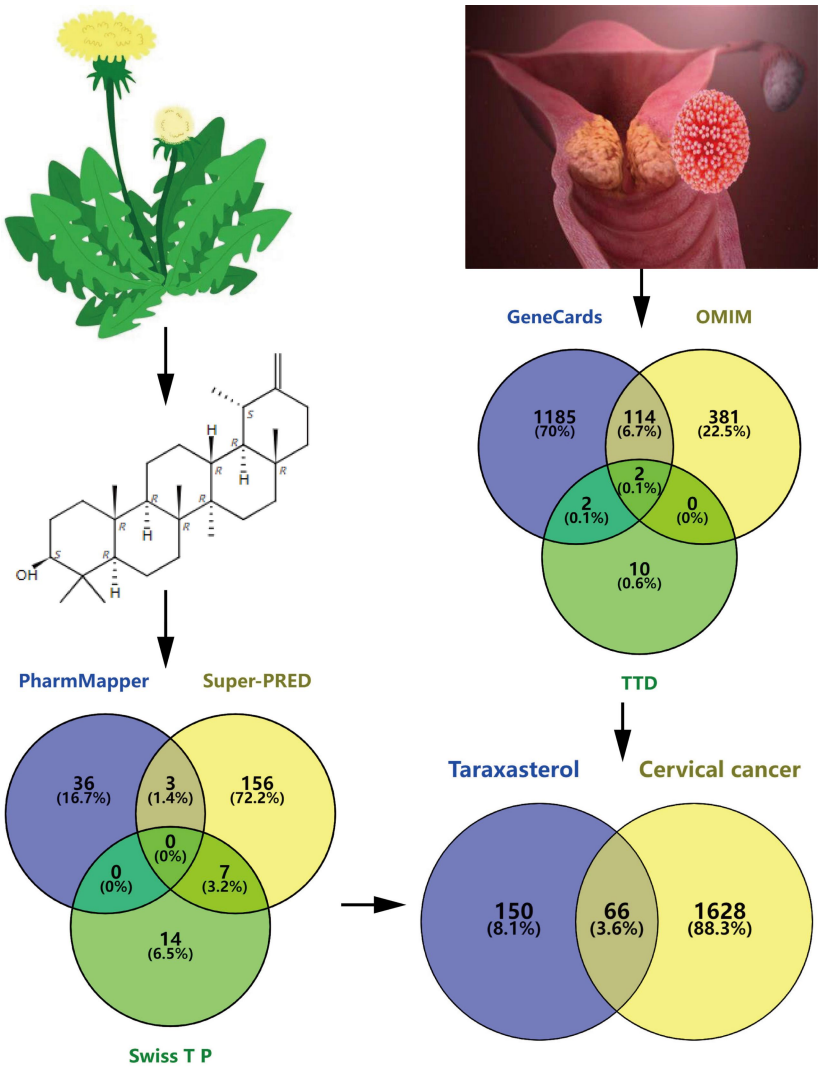

Figure 1 Shared targets screening of taraxasterol and cervical cancer

Table 1 Shared targets of taraxasterol and cervical cancer

Number	Gene symbol	Gene ID	Description
1	AKR1C3	8644	Aldo-Keto Reductase Family 1 Member C3
2	ALB	213	Albumin
3	ANXA5	308	Annexin A5
4	APEX1	328	Apurinic/Apyrimidinic Endodeoxyribonuclease 1
5	AR	367	Androgen Receptor
6	AURKB	9212	Aurora Kinase B
7	BCL6	604	Bcl6 Transcription Repressor
8	BLM	641	Blm Recq Like Helicase
9	BMP2	650	Bone Morphogenetic Protein 2
10	BRD4	23476	Bromodomain Containing 4
11	CASP7	840	Caspase 7
12	CCNE1	898	Cyclin E1
13	CDC25A	993	Cell Division Cycle 25A
14	CDC25C	995	Cell Division Cycle 25C
15	CDK1	983	Cyclin Dependent Kinase 1
16	CDK2	1017	Cyclin Dependent Kinase 2
17	CDK4	1019	Cyclin Dependent Kinase 4
18	CDK5	1020	Cyclin Dependent Kinase 5
19	CFTR	1080	Cf Transmembrane Conductance Regulator
20	CTSD	1509	Cathepsin D
21	CXCR4	7852	C-X-C Motif Chemokine Receptor 4
22	CYP19A1	1588	Cytochrome P450 Family 19 Subfamily A Member 1
23	CYP3A4	1576	Cytochrome P450 Family 3 Subfamily A Member 4
24	ESR1	2099	Estrogen Receptor 1
25	F2	2147	Coagulation Factor Ii, Thrombin
26	FLT3	2322	Fms Related Receptor Tyrosine Kinase 3
27	GSTP1	2950	Glutathione S-Transferase Pi 1
28	HDAC1	3065	Histone Deacetylase 1
29	HDAC2	3066	Histone Deacetylase 2
30	HDAC4	9759	Histone Deacetylase 4
31	HDAC9	9734	Histone Deacetylase 9
32	HPSE	10855	Heparanase
33	HSD17B1	3292	Hydroxysteroid 17-Beta Dehydrogenase 1
34	IDH1	3417	Isocitrate Dehydrogenase (NADP (+)) 1
35	IDO1	3620	Indoleamine 2,3-Dioxygenase 1
36	KDR	3791	Kinase Insert Domain Receptor
37	KEAP1	9817	Kelch Like Ech Associated Protein 1
38	KLF5	688	Klf Transcription Factor 5
39	MAPK1	5594	Mitogen-Activated Protein Kinase 1
40	MAPK14	1432	Mitogen-Activated Protein Kinase 14
41	MAPK8	5599	Mitogen-Activated Protein Kinase 8
42	MME	4311	Membrane Metalloendopeptidase
43	MMP13	4322	Matrix Metallopeptidase 13
44	NFKB1	4790	Nuclear Factor Kappa B Subunit 1
45	NTRK3	4916	Neurotrophic Receptor Tyrosine Kinase 3
46	PDGFRA	5156	Platelet Derived Growth Factor Receptor Alpha
47	PGR	5241	Progesterone Receptor
48	PIK3CB	5291	Phosphatidylinositol-4,5-Bisphosphate 3-Kinase Catalytic Subunit Beta
49	PIK3R1	5295	Phosphoinositide-3-Kinase Regulatory Subunit 1
50	PLA2G2A	5320	Phospholipase A2 Group Iia
51	PPARG	5468	Peroxisome Proliferator Activated Receptor Gamma
52	PRKAA1	5562	Protein Kinase Amp-Activated Catalytic Subunit Alpha 1
53	PRKCD	5580	Protein Kinase C Delta
54	PTGS1	5742	Prostaglandin-Endoperoxide Synthase 1
55	PTK2B	2185	Protein Tyrosine Kinase 2 Beta
56	PTPN11	5781	Protein Tyrosine Phosphatase Non-Receptor Type 11
57	SIRT1	23411	Sirtuin 1
58	STAT3	6774	Signal Transducer and Activator of Transcription 3
59	STS	412	Steroid Sulfatase
60	TERT	7015	Telomerase Reverse Transcriptase
61	TGFBR1	7046	Transforming Growth Factor Beta Receptor 1
62	TLR4	7099	Toll Like Receptor 4
63	TOP2A	7153	Dna Topoisomerase Ii Alpha
64	TRIM24	8805	Tripartite Motif Containing 24
65	TYMS	7298	Thymidylate Synthetase
66	VDR	7421	Vitamin D Receptor

"TS-cervical cancer-targets" network construction and hub targets selection

Using Cytoscape 3.8.0, the "TS-cervical cancer-targets" network was established and presented in Figure 2A. The STRING database (up to November 1, 2022) was employed to analyze PPI, and the PPI network was constructed and visualized using Cytoscape (Figure 2B). The degree values were utilized to determine the significance of the targets, with the 65 nodes in the PPI network represented by colored solid balls. The network produced 477 edges with an average neighbor of 14.68 (Figure 2B).

The 12 hub targets were obtained through selection criteria, and PPI was calculated using STRING, while the PPI network was visualized using Cytoscape (Figure 2C–D). The PPI network generated 12 nodes and 60 edges, with an average neighbor of 10 (Figure 2D). Signal transducer and activator of transcription 3 (STAT3) gained the highest degree of the 66 targets (degree = 43), followed by estrogen receptor 1 (ESR1, degree = 40) and albumin (ALB, degree = 38).

Targets clustering

The nodes and scores of the assigned clusters were plotted in (Figure 3A). Networks of clusters were generated using STRING predictions and visualized using Cytoscape (Figure 3B–D).

In Figure 3B, Cluster 1 comprised of 19 nodes and 100 edges, with an average neighbor of 10.53 and a score of 11.111. The seed node of Cluster 1 was PGR, which plays a crucial role in regulating eukaryotic gene expression, cellular proliferation, and differentiation [45]. Cluster 2, on the other hand, consisted of 15 nodes and 35 edges, with an average neighbor of 4.66 and a score of 5, as shown in Figure 3C. The seed node of Cluster 2 was steryl-sulfatase, which is responsible for catalyzing the conversion of sulfated steroid precursors to the free steroid [46]. Lastly, Cluster 3 contained 9 nodes and 16 edges, with an average neighbor of 3.56 and a score of 4, as depicted in Figure 3D. The seed node of Cluster 3 was mitogen-activated protein kinase 8, which primarily phosphorylates a number of transcription factors, particularly components of AP-1 [47].

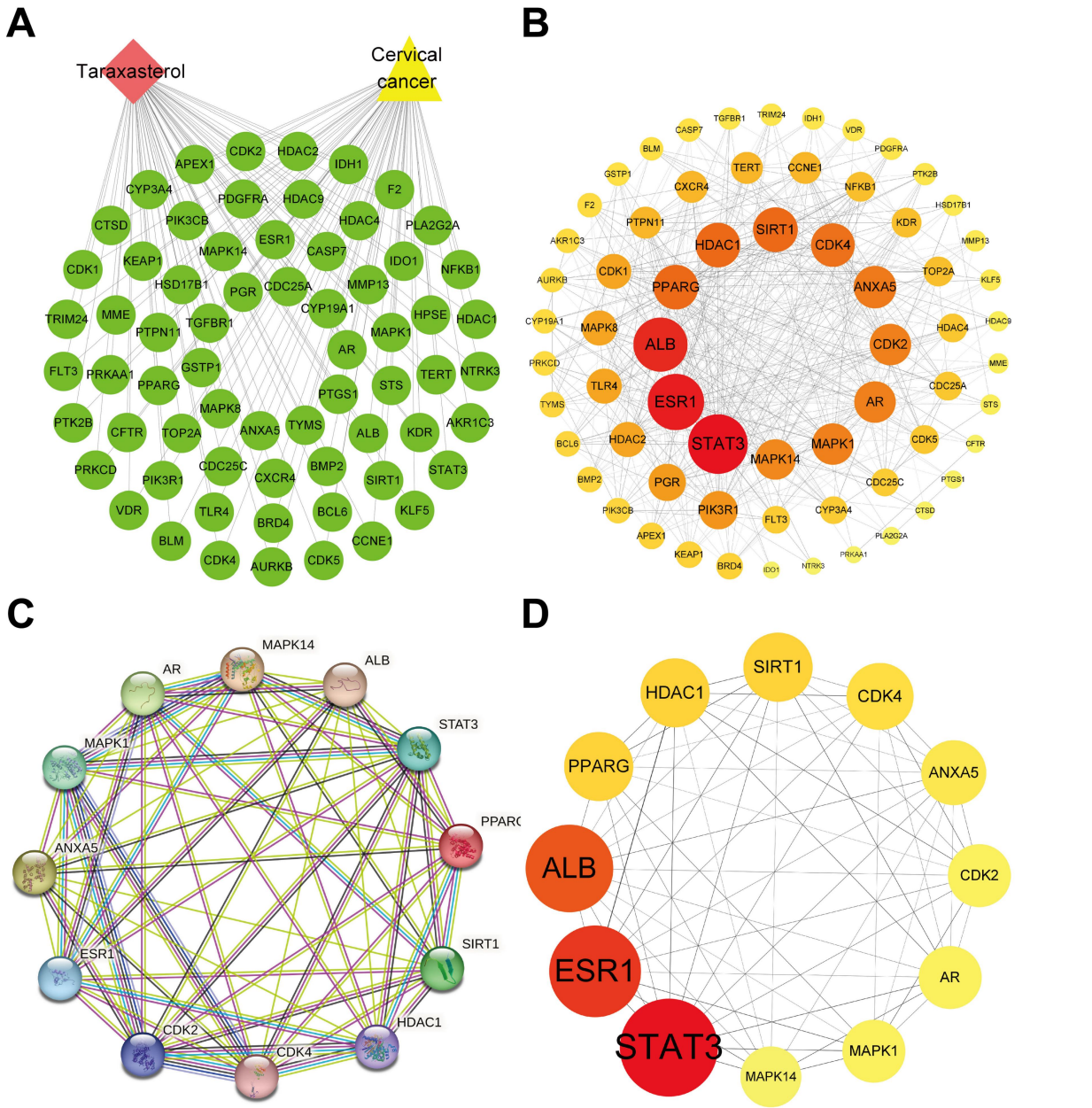

Figure 2 "Taraxasterol-Cervical Cancer-targets" network construction and hub targets selection. (A–B) "Taraxasterol-cervical cancer-targets" network; (C) Hub targets PPI network; (D) Visualization of hub targets PPI network. Nodes and lines represent the target proteins and interactions. The targets were ranked by degree value. The greater the degree is, the larger the node is. PPI, protein-protein interaction.

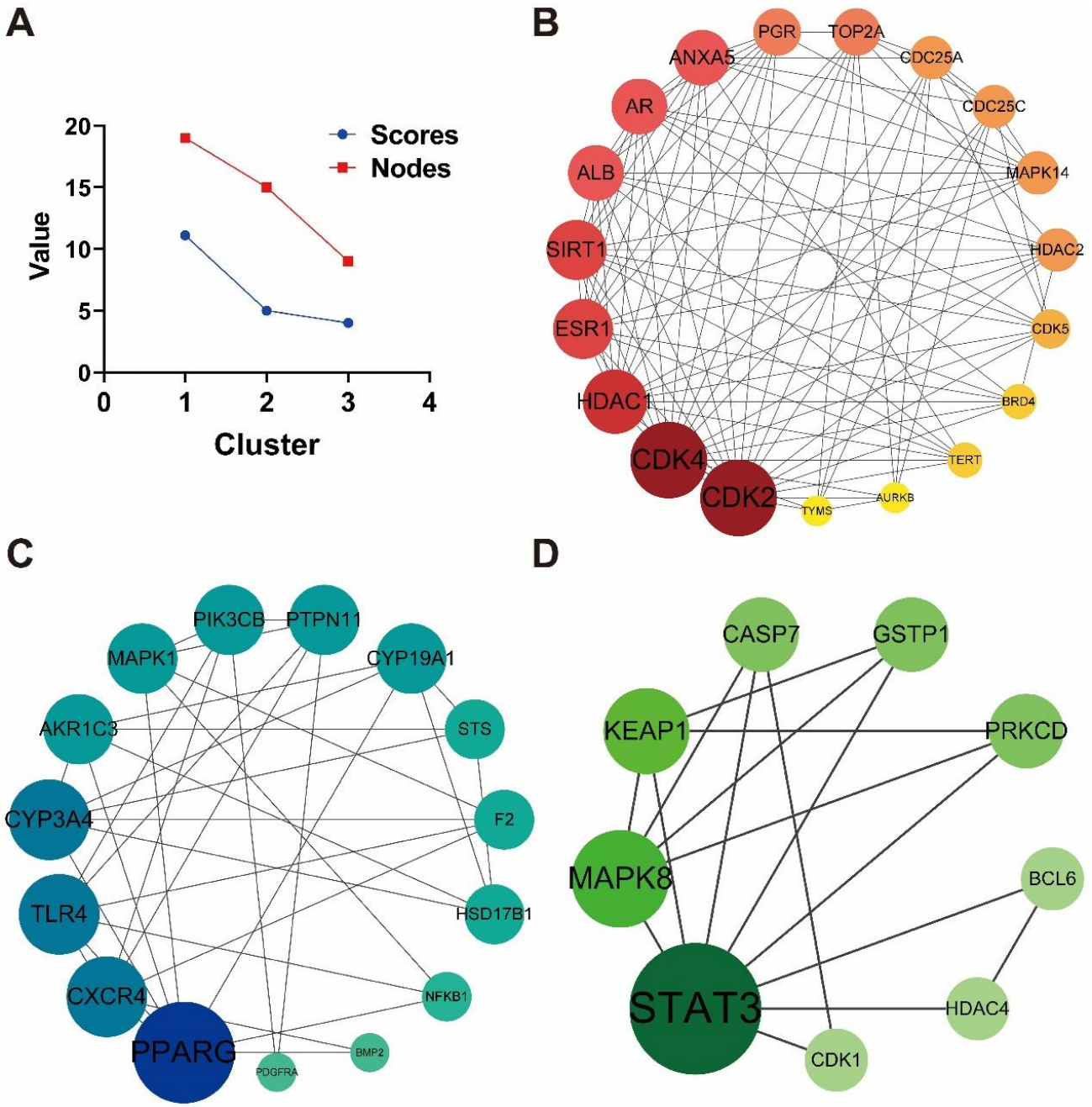

Figure 3 Clustering of the shared 66 targets. (A) Nodes and scores of different clusters were predicted by MCODE; (B–D) Visualization of the PPI networks of the three clusters. PPI, protein-protein interaction.

GO enrichment analysis

The top 20 enriched GO biological process terms with *P*-value < 0.001 were organized in (Figure 4A). Of the 20 terms, 6 were corelated with gene expression regulation, while the rest were associated with cell proliferation, protein phosphorylation, apoptotic process, cell migration, inflammation and histone deacetylation.

The top 20 molecular function terms, with a *P*-value < 0.001, were primarily associated with protein/kinase binding, enzyme binding, and receptor binding. These functions were mainly linked to cellular signaling transduction and gene expression (Figure 4B).

KEGG pathway enrichment analysis

The top 20 KEGG enriched pathways with *P*-value < 0.001 were selected (Figure 5A). Among the terms, 8 out of 20 were associated with cancer, which occupied 40% of the total. Cancer-related enrichment pathways were listed as follows: pathways in cancer (hsa05200), viral carcinogenesis (hsa05203), chemical carcinogenesis-receptor activation (hsa05207), prostate cancer (hsa05215), pancreatic cancer (hsa05212), chronic myeloid leukemia (hsa05220), microRNAs in cancer (hsa05206), and PD-L1 expression and PD-1 checkpoint pathway in cancer (hsa05235). Among the 20 terms, two pathways involved in female hormones are the prolactin signaling pathway (hsa04917) and progesterone-mediated oocyte maturation (hsa04914). Details of these enriched KEGG pathways are listed in (Table 2).

A "targets-pathways" network was constructed to better understand the relationships between the terms and target proteins (Figure 5B). The network had 63 nodes and 217 edges, with an average degree (neighbor) of 6.89.

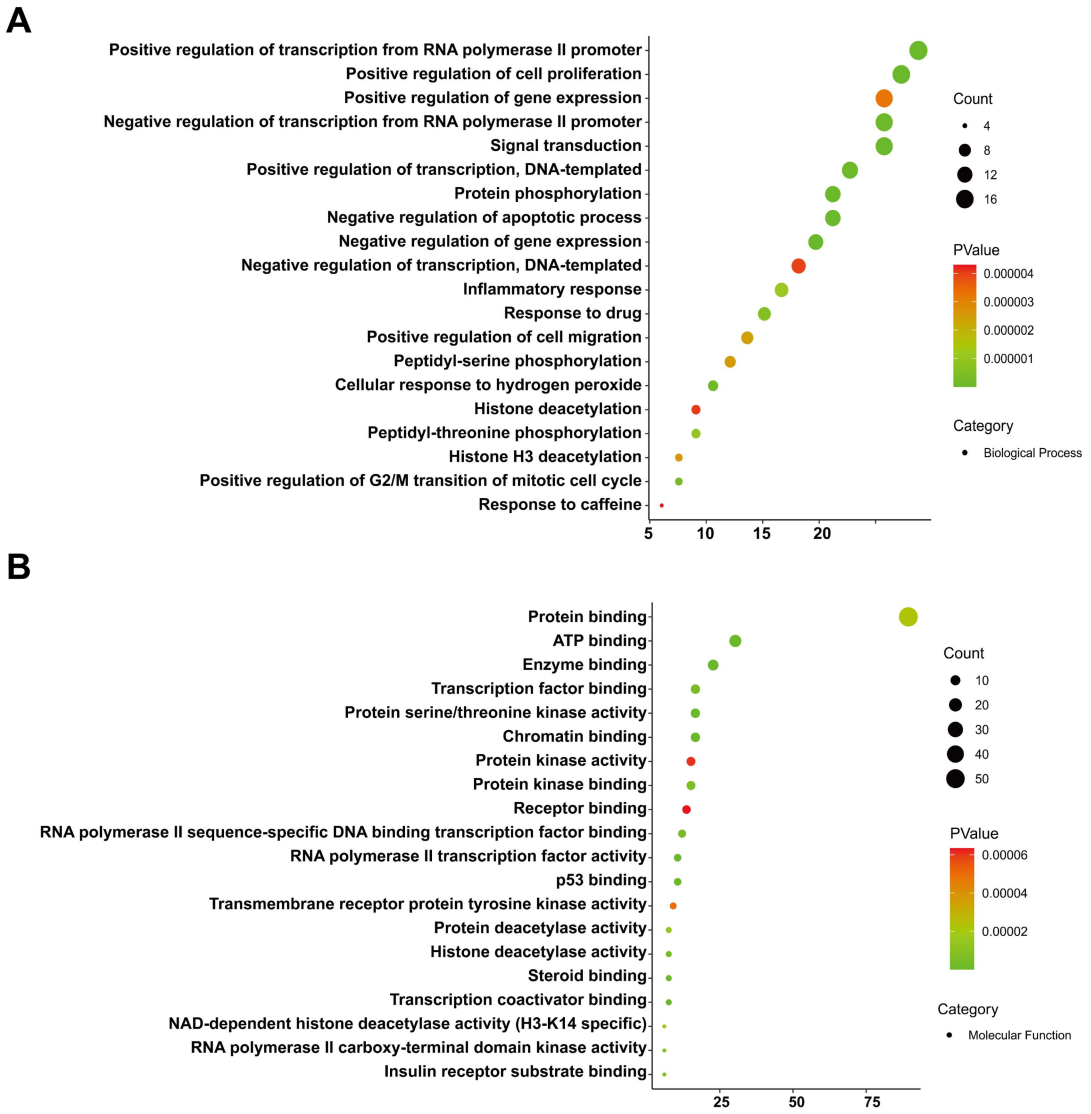

Figure 4 GO enrichment analysis of BP and MF. (A–B) Biological process and molecular function of the 66 targets. The bubble size represents the number of targets enriched in terms, and the bubble color indicates the *P*-value. GO, gene ontology; BP, biological process; MF, molecular functions.

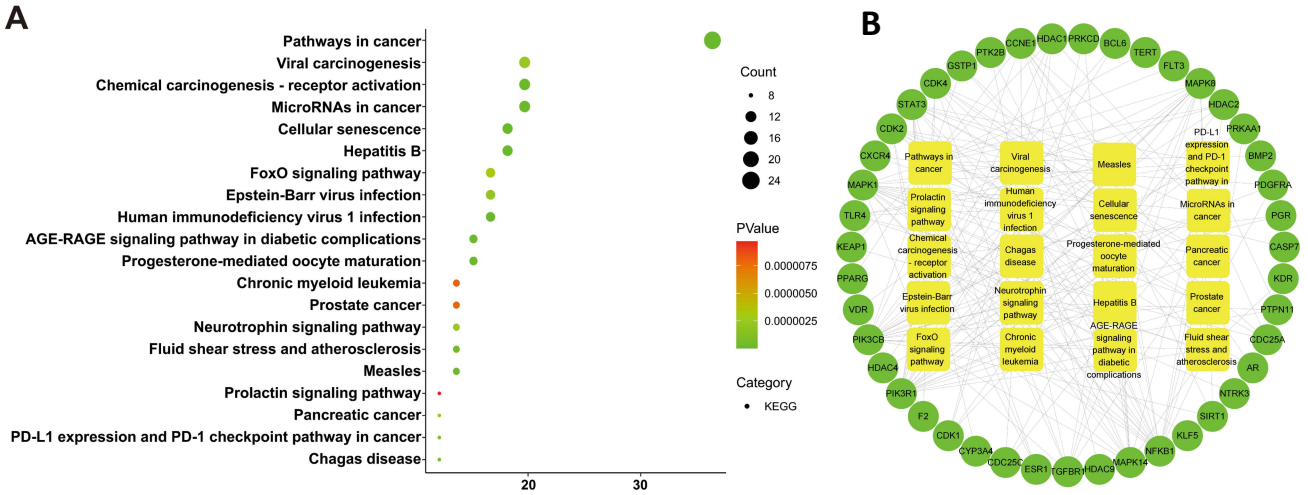

Figure 5 Targets enriched KEGG pathway network of taraxasterol against cancer. (A) The top 20 enriched KEGG pathways of the 66 targets; (B) Visualization of KEGG pathways and targets. The outer circle represents targets involved in pathways. The top 20 enriched KEGG pathways (*P*-value < 0.001) were represented using yellow squares. The line represents the involvement. KEGG, Kyoto Encyclopedia of Genes and Genomes.

Table 2 KEGG enrichment analysis of taraxasterol against cancer

Terms	Pathways	Count	*P*-Value	Ratio	Gene symbols
hsa05200	Pathways in cancer	24	1.16E-12	36.36363636	PDGFRA, HDAC2, FLT3, HDAC1, GSTP1, STAT3, CXCR4, KEAP1, PIK3CB, PIK3R1, F2, ESR1, TGFBR1, NFKB1, AR, CASP7, BMP2, MAPK8, TERT, CCNE1, CDK4, CDK2, MAPK1, PPARG
hsa04218	Cellular senescence	12	1.60E-08	18.18181818	CCNE1, CDK4, CDK2, CDK1, MAPK1, PIK3CB, PIK3R1, MAPK14, SIRT1, CDC25A, TGFBR1, NFKB1
hsa05161	Hepatitis B	12	2.37E-08	18.18181818	MAPK8, CCNE1, STAT3, CDK2, PTK2B, MAPK1, PIK3CB, PIK3R1, MAPK14, TLR4, TGFBR1, NFKB1
hsa05203	Viral carcinogenesis	13	2.55E-08	19.6969697	HDAC4, HDAC2, HDAC1, STAT3, PIK3CB, PIK3R1, HDAC9, NFKB1, CCNE1, CDK4, CDK2, CDK1, MAPK1
hsa04068	FoxO signaling pathway	11	3.61E-08	16.66666667	PRKAA1, MAPK8, BCL6, STAT3, CDK2, MAPK1, PIK3CB, PIK3R1, MAPK14, SIRT1, TGFBR1
hsa05207	Chemical carcinogenesis-receptor activation	13	3.92E-08	19.6969697	VDR, STAT3, PIK3CB, PIK3R1, CYP3A4, ESR1, CDC25A, NFKB1, AR, KLF5, BCL6, MAPK1, PGR
hsa04933	AGE-RAGE signaling pathway in diabetic complications	10	4.41E-08	15.15151515	MAPK8, CDK4, STAT3, PRKCD, MAPK1, PIK3CB, PIK3R1, MAPK14, TGFBR1, NFKB1
hsa04914	Progesterone-mediated oocyte maturation	10	5.25E-08	15.15151515	MAPK8, CDK2, CDK1, MAPK1, PGR, PIK3CB, PIK3R1, CDC25C, MAPK14, CDC25A
hsa05220	Chronic myeloid leukemia	9	7.67E-08	13.63636364	HDAC2, HDAC1, CDK4, MAPK1, PTPN11, PIK3CB, PIK3R1, TGFBR1, NFKB1
hsa05215	Prostate cancer	9	5.21E-07	13.63636364	PDGFRA, AR, CCNE1, GSTP1, CDK2, MAPK1, PIK3CB, PIK3R1, NFKB1
hsa04917	Prolactin signaling pathway	8	7.58E-07	12.12121212	MAPK8, STAT3, MAPK1, PIK3CB, PIK3R1, MAPK14, ESR1, NFKB1
hsa05212	Pancreatic cancer	8	1.34E-06	12.12121212	MAPK8, CDK4, STAT3, MAPK1, PIK3CB, PIK3R1, TGFBR1, NFKB1
hsa05169	Epstein-Barr virus infection	11	2.07E-06	16.66666667	HDAC2, MAPK8, CCNE1, HDAC1, CDK4, STAT3, CDK2, PIK3CB, PIK3R1, MAPK14, NFKB1
hsa05206	MicroRNAs in cancer	13	2.38E-06	19.6969697	HDAC4, PDGFRA, HDAC2, HDAC1, STAT3, PIK3CB, PIK3R1, CDC25C, SIRT1, CDC25A, NFKB1, CCNE1, MAPK1
hsa04722	Neurotrophin signaling pathway	9	2.49E-06	13.63636364	MAPK8, NTRK3, PRKCD, MAPK1, PTPN11, PIK3CB, PIK3R1, MAPK14, NFKB1
hsa05170	Human immunodeficiency virus 1 infection	11	3.20E-06	16.66666667	MAPK8, CDK1, PTK2B, MAPK1, CXCR4, PIK3CB, PIK3R1, CDC25C, MAPK14, TLR4, NFKB1
hsa05235	PD-L1 expression and PD-1 checkpoint pathway in cancer	8	3.90E-06	12.12121212	STAT3, MAPK1, PTPN11, PIK3CB, PIK3R1, MAPK14, TLR4, NFKB1
hsa05418	Fluid shear stress and atherosclerosis	9	7.94E-06	13.63636364	PRKAA1, MAPK8, GSTP1, KDR, KEAP1, PIK3CB, PIK3R1, MAPK14, NFKB1
hsa05162	Measles	9	7.94E-06	13.63636364	MAPK8, CCNE1, CDK4, STAT3, CDK2, PIK3CB, PIK3R1, TLR4, NFKB1
hsa05142	Chagas disease	8	9.70E-06	12.12121212	MAPK8, MAPK1, PIK3CB, PIK3R1, MAPK14, TLR4, TGFBR1, NFKB1

KEGG, Kyoto Encyclopedia of Genes and Genomes.

Molecular docking validation

Of the 12 hub targets, nine can interact with TS through molecular docking analysis, with affinity energy < − 5.0 kcal/mol, which indicated strong interaction between TS and hub targets. 2D and 3D binding structures of the top 4 were selected and shown in (Figure 6 A–D). More details of the nine binding complexes are listed in (Table 3).

Expression and overall survival analysis

Expression patterns were analyzed using Sanger-box 3.0 and shown in (Figure 7). We observed significant up-regulation of histone deacetylase 1 (HDAC1) and down-regulation of the estrogen receptor 1 (ESR1) and androgen receptor (AR) in cervical squamous cell carcinoma and endocervical adenocarcinoma (Figure 7A, Figure 7E, Figure 7G). No significant difference was observed in mitogen-activated protein kinase 1 (MAPK1) (Figure 7C).

Overall survival analysis was performed through GEPIA (Figure 7, right panel). During the first 100 months, no differences were observed in ESR1 expression, but after that time, high ESR1 expression led to a lower survival percent (Figure 7B). MAPK1 expression level did not influence the survival percent, which was parallel with the pan-cancer analysis result (Figure 7B–C). High expression of HDAC1 and AR led to a lower survival percent, especially after 100 months (Figure 7F–H).

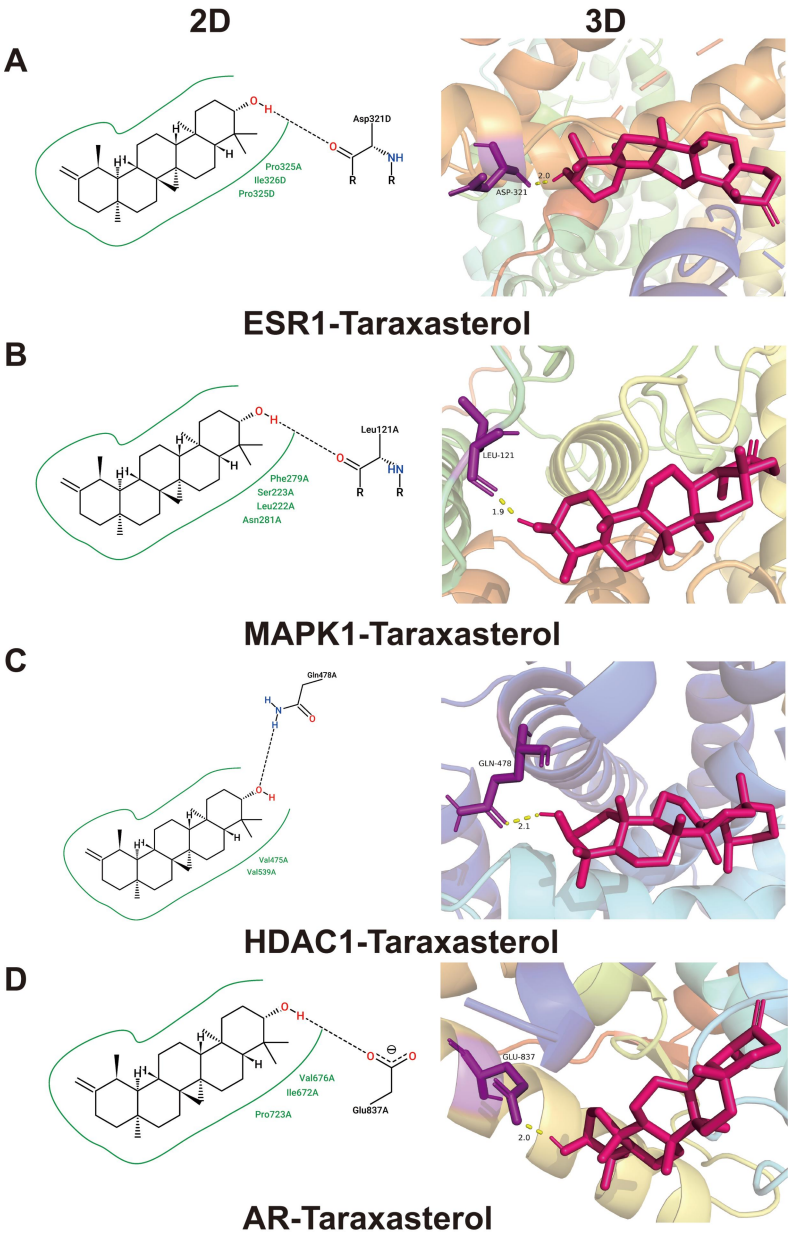

Figure 6 Molecular docking between taraxasterol and hub targets. (A) 2D and 3D interacted structures of ESR1 and Taraxasterol; (B) 2D and 3D interacted structures of MAPK1 and Taraxasterol; (C) 2D and 3D interacted structures of HDAC1 and Taraxasterol; (D) 2D and 3D interacted structures of AR and Taraxasterol. ESR1, estrogen receptor 1; MAPK1, mitogen-activated protein kinase 1; HDAC1, histone deacetylase 1; AR, androgen receptor.

Table 3 Molecular docking between taraxasterol and the hub targets

No	Gene name	PDB ID	Interacted amino acids	No of H-bond	Distances of the H-bond (Å)	Affinity energy (kcal/mol)
1	ESR1	7UJW	ASP-321	1	2.0	−8.73
2	MAPK1	7E75	LEU-121	1	1.9	−8.07
3	HDAC1	7SMF	GLN-478	1	2.1	−7.95
4	AR	4QL8	GLU-837	1	2.0	−7.88
5	CDK2	6SG4	GLU-278	1	2.1	−7.61
6	ALB	6JE7	LEU-112	1	2.0	−7.57
7	ANXA5	6K22	GLU-191	1	2.1	−7.56
8	STAT3	6UNQ	ASP-173	1	1.9	−7.16
9	CDK4	6P8H	GLU-53	1	2.3	−6.92

ESR1, estrogen receptor 1; MAPK1, mitogen-activated protein kinase 1; HDAC1, histone deacetylase 1; AR, androgen receptor.

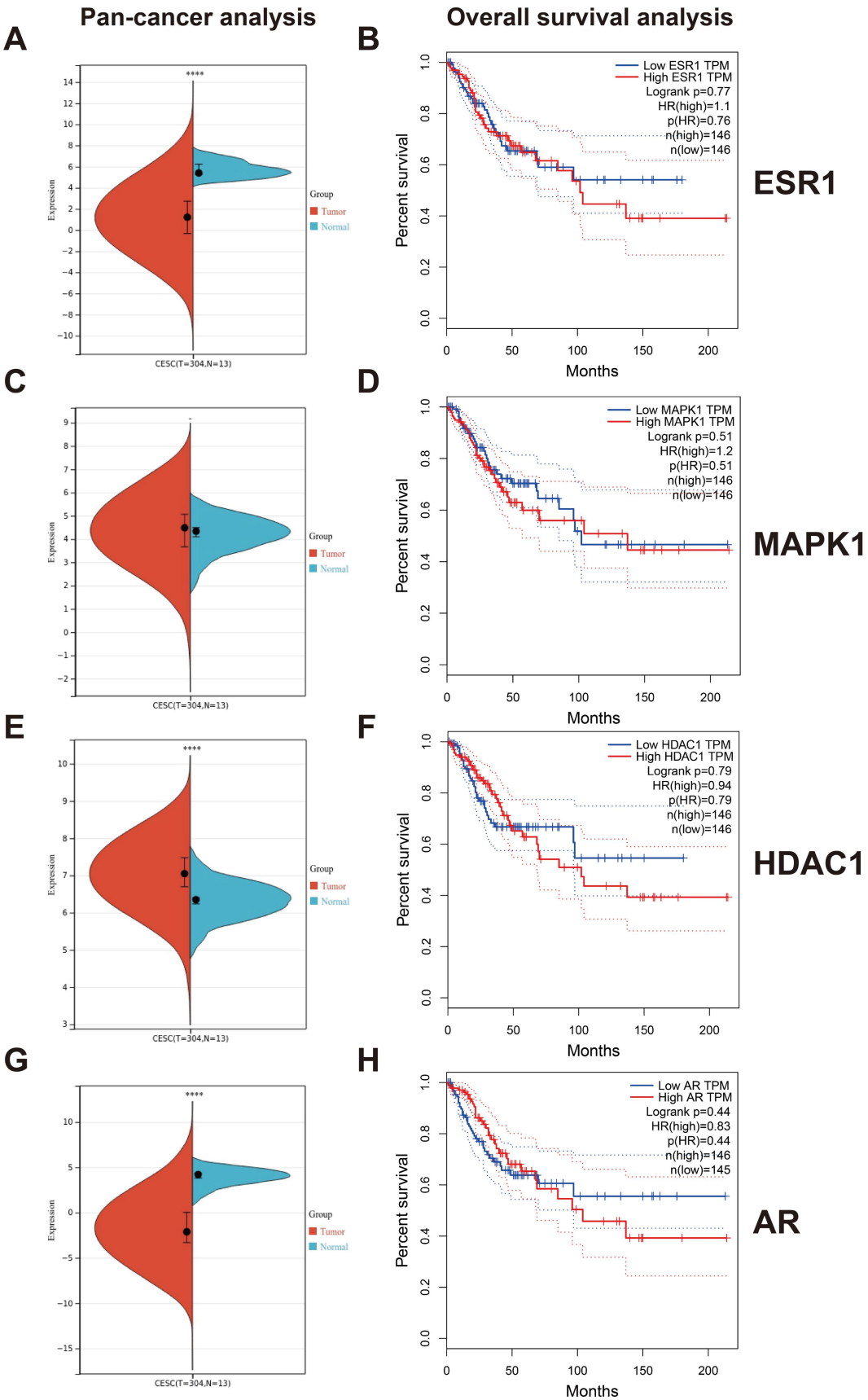

Figure 7 Expression pattern and overall survival analysis of ESR1, MAPK1, HDAC1, and AR in CESC. (A) Expression pattern and overall survival analysis of ESR1 in CESC; (B) Expression pattern and overall survival analysis of MAPK1 in CESC; (C) Expression pattern and overall survival analysis of HDAC1 in CESC; (D) Expression pattern and overall survival analysis of AR in CESC. ESR1, estrogen receptor 1; MAPK1, mitogen-activated protein kinase 1; HDAC1, histone deacetylase 1; AR, androgen receptor.

Cell viability analysis

To further prove the significant roles of TS in cervical cancer cells, cell viability had been assessed through MTT analysis. Different concentrations and time courses were set up, and after being treated with 0.5 μg/mL TS for 24 hours, cell viability alleviated significantly (Figure 8A–B). The TS treated concentration was proportionately increased, from 2.5 to 20 μg/mL, however, no visible difference was detected (Figure 8C–E). The statistical analysis was done and shown in (Figure 8D–F).

Cell migration assay

To test the influence of TS on cell migration, a wound healing assay was done. After being treated with 15 μg/mL TS for 24, 48, and 72 hours, migration rates were calculated. In contrast to the control group, TS treated cells had significantly poorer wound healing (Figure 9A–C).

Colony-forming assay

After being treated with 15 μg/mL TS for 7 days, cell colonies were fixed, stained, photographed, and calculated (Figure 10A). To further check the impact of TS on colony-forming, pictures were magnified and shown in (Figure 10B). Compared with the control group, cells treated with TS were harder to form colonies and more earsily to disperse (Figure 10B). Significant differences were obtained through colony counting (Figure 10 C).

Discussion

According to GLOBOCAN 2020 statistical data, cervical cancer ranks fourth in both incidence and mortality among females. It poses a massive threat to women's health, and more effective therapies are urgently needed [1].

In this study, 66 shared targets of TS and cervical cancer were identified for further investigation. The "TS-targets-cervical cancer" network revealed well-established relationships between TS and cervical cancer. Based on clustering analysis, three distinct clusters with different functions were constructed. The clusters demonstrated distinct anti-cancer effects of TS. The biological process analysis indicated that the shared targets were primarily associated with gene expression, cell proliferation, signal transduction, protein phosphorylation, cell migration, and apoptosis. Molecular function analysis revealed that these targets were linked with ATP binding, enzyme binding, transcription factor binding, and kinase activity. Furthermore, 40% of the KEGG enriched pathways corresponded to cancer, underscoring the significant anti-cancer roles that TS can play.

Molecular docking was performed between TS and 12 hub targets. Out of the 12 targets, 9 exhibited strong interaction with TS, with affinity scores below − 5 kcal/mol, indicating a robust binding affinity between the targets and TS.

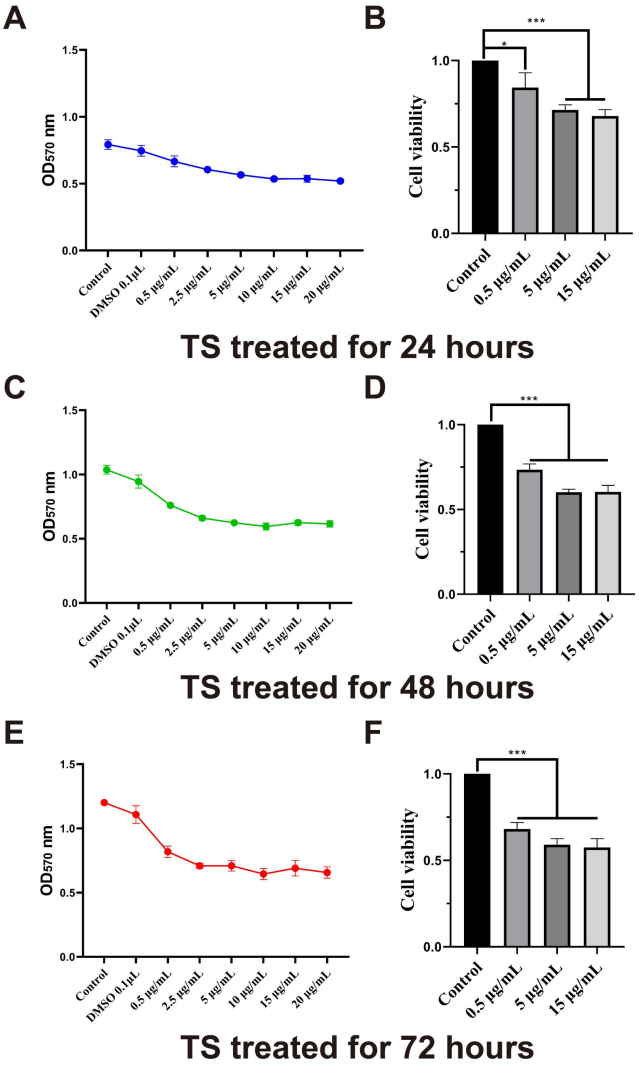

Figure 8 Cell viability assay. (A&C&E) Cell viability assay through MTT. HeLa-S3 cells were treated with different concentrations of taraxasterol for 24, 48, and 72 hours, respectively; (B&D&F) Statistical analysis between the control and TS treated groups. TS, Taraxasterol.

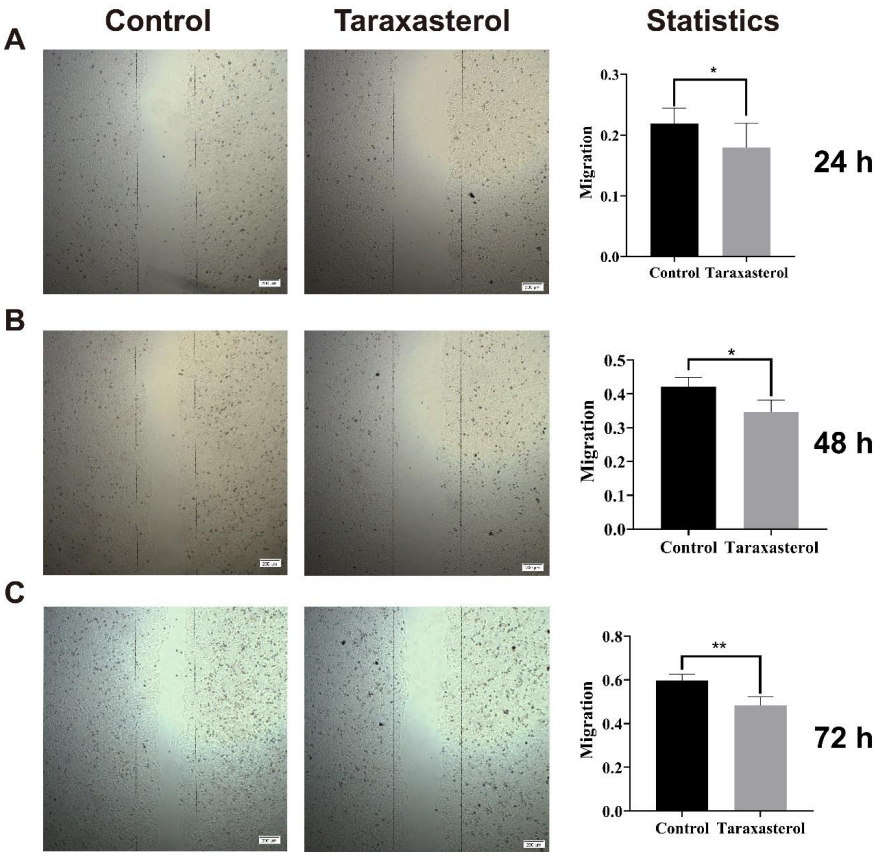

Figure 9 Cell migration assay. (A–C) Wound healing analysis and statistics. The bars labeled in the photos were 200 μm.

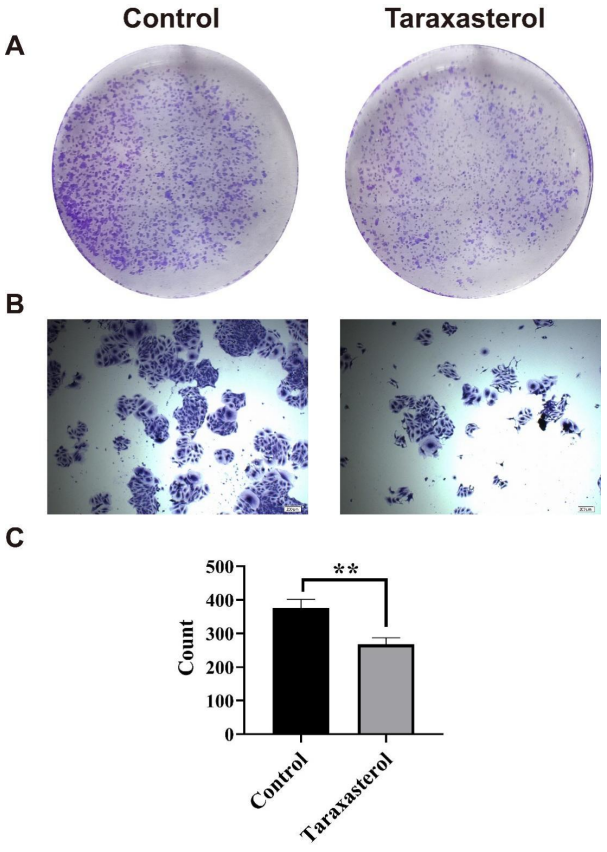

Figure 10 Colony-forming assay. (A) Cell colony formation assay; (B) The zoom-in pictures of control and taraxasterol treated cells. (C) The bars labeled in the photos were 200 μm.

In order to achieve this objective, an analysis of pan-cancer and overall survival was conducted based on four selected targets: ESR1, MAPK1, HDAC1, and AR. ESR1 is an estrogen receptor that regulates the expression of eukaryotic genes and contributes to cellular proliferation and differentiation upon binding to steroid hormones [48]. MAPK1 plays a significant role in the MAPK/ERK cascade, which regulates various biological functions such as cell growth, adhesion, survival, and differentiation by controlling transcription, translation, and cytoskeletal rearrangements [49, 50]. HDAC1 catalyzes the deacetylation of lysine residues on the N-terminal region of the core histones, which creates an epigenetic repression tag and is crucial in regulating transcription, cell cycle progression, and developmental events [51]. Similar to ESR1, AR also binds to steroid hormones and mediates eukaryotic gene expression, cell proliferation, and differentiation in target tissues [52]. Moreover, together with the illustrated core targets, these hub targets played significant roles in cell growth, proliferation, migration, invasion, adhesion, and apoptosis, transcriptional regulation, and cell cycle [53–55].

The pan-cancer and overall survival analyses of hub targets indicated the significant anti-cancer effects of TS, particularly in cervical cancer. To further substantiate this hypothesis, in vitro experiments were conducted. The MTT analysis showed that TS effectively inhibited cell growth. Moreover, through cell migration and colony-forming assays, it was observed that TS suppressed cell migration. Additionally, cell apoptosis was analyzed via flow cytometry in HeLa-S3 cells following TS treatment, but no significant difference was observed (data not shown).

TS has potent anti-inflammatory and anti-tumor activity, and it can strongly impede the proliferation, growth, and migration of cells. The anti-cancer effect of TS is mediated through various targets, pathways, and biological processes.

Conclusion

In our study, we employed a network-based pharmacology approach, molecular docking, and in vitro experimental validation to elucidate the anti-cancer effect of TS. GO enrichment and KEGG pathway analysis indicated that TS exerts an antagonistic effect on cervical cancer by regulating cellular processes such as cell proliferation, gene expression, protein kinase activity, and transcription. In vitro experiments provided confirmation of the inhibitory effects of TS on cell proliferation, growth, and migration. In summary, our report introduces a significant and valuable naturally occurring lead compound that demonstrates a potent anti-cancer effect in cervical cancer.

References

1. Sung H, Ferlay J, Siegel RL, et al. Global Cancer Statistics 2020: GLOBOCAN Estimates of Incidence and Mortality Worldwide for 36 Cancers in 185 Countries. *CA A Cancer J Clin* 2021;71(3):209–249. Available at: http://doi.org/10.3322/caac.21660
2. Global Burden of Disease Cancer Collaboration, Fitzmaurice C, Dicker D, et al. The Global Burden of Cancer 2013. *JAMA Oncol* 2015;1(4):505–527. Available at: http://doi.org/10.1001/jamaoncol.2015.0735
3. Vineis P, Wild CP. Global cancer patterns: causes and prevention. *Lancet* 2014;383(9916):549–557. Available at: http://doi.org/10.1016/S0140-6736(13)62224-2
4. Yin XJ, Xu Y, Man XW, et al. Direct costs of both inpatient and outpatient care for all type cancers: The evidence from Beijing, China. *Cancer Med* 2019;8(6):3250–3260. Available at: http://doi.org/10.1002/cam4.2184
5. Huang HY, Shi JF, Guo LW, et al. Expenditure and financial burden for common cancers in China: a hospital-based multicentre cross-sectional study. *Chin J Cancer* 2017;36(1):41. Available at: http://doi.org/10.1016/S0140-6736(16)31937-7
6. Wu WY, Zhang ZJ, Li FF, et al. A Network-Based Approach to Explore the Mechanisms of Uncaria Alkaloids in Treating Hypertension and Alleviating Alzheimer's Disease. *Int J Mol Sci* 2020;21(5):1766. Available at: http://doi.org/10.3390/ijms21051766
7. Xie JM, Chen RX, Wang QZ, Mao H. Exploration and validation of Taraxacum mongolicum anti-cancer effect. *Comput Biol Med* 2022;148:105819. Available at: http://doi.org/10.1016/j.compbiomed.2022.105819
8. Li XH, He XR, Zhou YY, et al. Taraxacum mongolicum extract induced endoplasmic reticulum stress associated-apoptosis in triple-negative breast cancer cells. *J Ethnopharmacol* 2017;206:55–64. Available at: http://doi.org/10.1016/j.jep.2017.04.025
9. Ren F, Wu KX, Yang Y, Yang YY, Wang YX, Li J. Dandelion Polysaccharide Exerts Anti-Angiogenesis Effect on Hepatocellular Carcinoma by Regulating VEGF/HIF-1α Expression. *Front Pharmacol* 2020;11:460. Available at: http://doi.org/10.3389/fphar.2020.00460
10. Xu HY, Zhang YQ, Liu ZM, et al. ETCM: an encyclopaedia of traditional Chinese medicine. *Nucleic Acids Res* 2018;47(D1):D976–982. Available at: http://doi.org/10.1093/nar/gky987
11. Zeng X, Zhang P, He WD, et al. NPASS: natural product activity and species source database for natural product research, discovery and tool development. *Nucleic Acids Res* 2017;46(D1):D1217–1222. Available at: http://doi.org/10.1093/nar/gkx1026
12. Zhang Y, Hu YF, Li W, et al. Updates and advances on pharmacological properties of Taraxacum mongolicum Hand.-Mazz and its potential applications. *Food Chem* 2022;373:131380. Available at: http://doi.org/10.1016/j.foodchem.2021.131380
13. Duan XF, Pan LM, Deng YY, et al. Dandelion root extract affects ESCC progression via regulating multiple signal pathways. *Food Funct* 2021;12(19):9486–9502. Available at: http://doi.org/10.1039/D1FO01093J
14. Kang L, Miao MS, Song YG, et al. Total flavonoids of Taraxacum mongolicum inhibit non-small cell lung cancer by regulating immune function. *J Ethnopharmacol* 2021;281:114514. Available at: http://doi.org/10.1016/j.jep.2021.114514
15. González-Castejón M, Visioli F, Rodriguez-Casado A. Diverse biological activities of dandelion. *Nutr Rev* 2012;70(9):534–547. Available at: http://doi.org/10.1111/j.1753-4887.2012.00509.x
16. Ru JL, Li P, Wang JN, et al. TCMSP: a database of systems pharmacology for drug discovery from herbal medicines. *J Cheminform* 2014;6:13. Available at: http://doi.org/10.1186/1758-2946-6-13
17. Ye XJ, Xu R, Liu SY, et al. Taraxasterol mitigates Con A-induced hepatitis in mice by suppressing interleukin-2 expression and its signaling in T lymphocytes. *Int Immunopharmacol* 2022;102:108380. Available at: http://doi.org/10.1016/j.intimp.2021.108380
18. Ren F, Zhang Y, Qin YH, et al. Taraxasterol prompted the anti-tumor effect in mice burden hepatocellular carcinoma by regulating T lymphocytes. *Cell Death Discov* 2022;8(1):264. Available at: http://doi.org/10.1038/s41420-022-01059-5
19. Liu WF, Yu QY, Wang F, Li YX, Zhang GH, Tao SR. Taraxasterol attenuates melanoma progression via inactivation of reactive oxygen species-mediated PI3K/Akt signaling pathway. *Hum Exp Toxicol* 2022;41:9603271211069034. Available at: http://doi.org/10.1177/09603271211069034
20. Zhao Y, Zhang L, Guo M, Yang HX. Taraxasterol suppresses cell proliferation and boosts cell apoptosis via inhibiting GPD2-mediated glycolysis in gastric cancer. *Cytotechnology* 2021;73(6):815–825. Available at:

http://doi.org/10.1007/s10616-021-00499-8
21. Yang F, Ye XJ, Chen MY, et al. Inhibition of NLRP3 Inflammasome Activation and Pyroptosis in Macrophages by Taraxasterol Is Associated With Its Regulation on mTOR Signaling. *Front Immunol* 2021;12:632606. Available at: http://doi.org/10.3389/fimmu.2021.632606
22. Tang CT, Yang J, Liu ZD, Chen YX, Zeng CY. Taraxasterol acetate targets RNF31 to inhibit RNF31/p53 axis-driven cell proliferation in colorectal cancer. *Cell Death Discov* 2021;7(1):66. Available at: http://doi.org/10.1038/s41420-021-00449-5
23. Daina A, Michielin O, Zoete V. SwissADME: a free web tool to evaluate pharmacokinetics, drug-likeness and medicinal chemistry friendliness of small molecules. *Sci Rep* 2017;7(1):42717. Available at: http://doi.org/10.1038/srep42717
24. Lipinski CA. Lead- and drug-like compounds: the rule-of-five revolution. *Drug Discov Today Technol* 2004;1(4):337–341. Available at: http://doi.org/10.1016/j.ddtec.2004.11.007
25. Daina A, Michielin O, Zoete V. SwissTargetPrediction: updated data and new features for efficient prediction of protein targets of small molecules. *Nucleic Acids Res* 2019;47(W1):W357–W364. Available at: http://doi.org/10.1093/nar/gkz382
26. Nickel J, Gohlke BO, Erehman J, et al. SuperPred: update on drug classification and target prediction. *Nucleic Acids Res* 2014;42(W1):W26–31. Available at: http://doi.org/10.1093/nar/gku477
27. Wang X, Shen YH, Wang SW, et al. PharmMapper 2017 update: a web server for potential drug target identification with a comprehensive target pharmacophore database. *Nucleic Acids Res* 2017;45(W1):W356–W360. Available at: http://doi.org/10.1093/nar/gkx374
28. Stelzer G, Rosen N, Plaschkes I, et al. The GeneCards Suite: From Gene Data Mining to Disease Genome Sequence Analyses. *Curr Protoc Bioinformatics* 2016;54:1.30.1–1.30.33. Available at: http://doi.org/10.1002/cpbi.5
29. Hamosh A. Online Mendelian Inheritance in Man (OMIM), a knowledgebase of human genes and genetic disorders. *Nucleic Acids Res* 2005;33(Database issue):D514–D517. Available at: http://doi.org/10.1093/nar/gki033
30. Zhou Y, Zhang YT, Lian XC, et al. Therapeutic target database update 2022: facilitating drug discovery with enriched comparative data of targeted agents. *Nucleic Acids Res* 2021;50(D1):D1398–D1407. Available at: http://doi.org/10.1093/nar/gkab953
31. Shannon P, Markiel A, Ozier O, et al. Cytoscape: A Software Environment for Integrated Models of Biomolecular Interaction Networks. *Genome Res* 2003;13(11):2498–2504. Available at: http://doi.org/10.1101/gr.1239303
32. Szklarczyk D, Gable AL, Nastou KC, et al. The STRING database in 2021: customizable protein–protein networks, and functional characterization of user-uploaded gene/measurement sets. *Nucleic Acids Res* 2020;49(D1):D605–D612. Available at: http://doi.org/10.1093/nar/gkaa1074
33. Wang L, Li H, Shen X, et al. Elucidation of the molecular mechanism of Sanguisorba Officinalis L. against leukopenia based on network pharmacology. *Biomed Pharmacother* 2020;132:110934. Available at: http://doi.org/10.1016/j.biopha.2020.110934
34. Zeng P, Wang XM, Ye CY, Su HF, Tian Q. The Main Alkaloids in Uncaria rhynchophylla and Their Anti-Alzheimer's Disease Mechanism Determined by a Network Pharmacology Approach. *Int J Mol Sci* 2021;22(7):3612. Available at: http://doi.org/10.3390/ijms22073612
35. Yu SX, Gao WH, Zeng PH, et al. Exploring the effect of Gupi Xiaoji Prescription on hepatitis B virus-related liver cancer through network pharmacology and in vitro experiments. *Biomed Pharmacother* 2021;139:111612. Available at: http://doi.org/10.1016/j.biopha.2021.111612
36. Bader GD, Hogue CWV. An automated method for finding molecular complexes in large protein interaction networks. *BMC Bioinformatics* 2003;4 (1):2. Available at: http://doi.org/10.1186/1471-2105-4-2
37. Huang DW, Sherman BT, Lempicki RA. Systematic and integrative analysis of large gene lists using DAVID bioinformatics resources. *Nat Protoc* 2008;4(1):44–57. Available at: http://doi.org/10.1038/nprot.2008.211
38. Huang DW, Sherman BT, Tan Q, et al. DAVID Bioinformatics Resources: expanded annotation database and novel algorithms to better extract biology from large gene lists. *Nucleic Acids Res* 2007;35(Web Server issue):W169–W175. Available at: http://doi.org/10.1093/nar/gkm415
39. Chen T, Liu YX, Huang LQ. ImageGP: An easy-to-use data visualization web server for scientific researchers. *iMeta* 2022;1(1). Available at: http://doi.org/10.1002/imt2.5
40. Trott O, Olson AJ. AutoDock Vina: Improving the speed and accuracy of docking with a new scoring function, efficient optimization, and multithreading. *J Comput Chem* 2010;31(2):455–461. Available at: http://doi.org/10.1002/jcc.21334
41. Morris GM, Huey R, Lindstrom W, et al. AutoDock4 and AutoDockTools4: Automated docking with selective receptor flexibility. *J Comput Chem* 2009;30(16):2785–2791. Available at: http://doi.org/10.1002/jcc.21256
42. Schöning-Stierand K, Diedrich K, Fährrolfes R, et al. ProteinsPlus: interactive analysis of protein–ligand binding interfaces. *Nucleic Acids Res* 2020;48(W1):W48–W53. Available at: http://doi.org/10.1093/nar/gkaa235
43. Liu FZ, Li YB, Yang Y, et al. Study on mechanism of matrine in treatment of COVID-19 combined with liver injury by network pharmacology and molecular docking technology. *Drug Deliv* 2021;28(1):325–342. Available at: http://doi.org/10.1080/10717544.2021.1879313
44. Tang ZF, Li CW, Kang BX, Gao G, Li C, Zhang ZM. GEPIA: a web server for cancer and normal gene expression profiling and interactive analyses. *Nucleic Acids Res* 2017;45(W1):W98–W102. Available at: http://doi.org/10.1093/nar/gkx247
45. Giangrande PH, Pollio G, McDonnell DP. Mapping and Characterization of the Functional Domains Responsible for the Differential Activity of the A and B Isoforms of the Human Progesterone Receptor. *J Biol Chem* 1997;272(52):32889–32900. Available at: http://doi.org/10.1074/jbc.272.52.32889
46. Alperin ES, Shapiro LJ. Characterization of Point Mutations in Patients with X-linked Ichthyosis. *J Biol Chem* 1997;272(33):20756–20763. Available at: http://doi.org/10.1074/jbc.272.33.20756
47. Murata T, Shinozuka Y, Obata Y, Yokoyama KK. Phosphorylation of two eukaryotic transcription factors, Jun dimerization protein 2 and activation transcription factor 2, in Escherichia coli by Jun N-terminal kinase 1. *Anal Biochem* 2008;376(1):115–121. Available at: http://doi.org/10.1016/j.ab.2008.01.038
48. Heldring N, Isaacs GD, Diehl AG, et al. Multiple Sequence-Specific DNA-Binding Proteins Mediate Estrogen Receptor Signaling through a Tethering Pathway. *Mol Endocrinol* 2011;25(4):564–574. Available at: http://doi.org/10.1210/me.2010-0425
49. Hu SH, Xie Z, Onishi A, et al. Profiling the human protein-DNA interactome reveals ERK2 as a transcriptional repressor of interferon signaling. *Cell* 2009;139(3):610–622. Available at:

http://doi.org/10.1016/j.cell.2009.08.037
50. Keyse SM. Protein phosphatases and the regulation of mitogen-activated protein kinase signalling. *Curr Opin Cell Biol* 2000;12(2):186–192. Available at: http://doi.org/10.1016/S0955-0674(99)00075-7
51. Qiu Y, Zhao YM, Becker M, et al. HDAC1 Acetylation Is Linked to Progressive Modulation of Steroid Receptor-Induced Gene Transcription. *Mol Cell* 2006;22(5):669–679. Available at: http://doi.org/10.1016/j.molcel.2006.04.019
52. Yang J, Zhao YL, Wu ZQ, et al. The single-macro domain protein LRP16 is an essential cofactor of androgen receptor. *Endocr Relat Cancer* 2009;16(1):139–153. Available at: http://doi.org/10.1677/ERC-08-0150
53. Harbour JW, Luo RX, Santi AD, Postigo AA, Dean DC. Cdk Phosphorylation Triggers Sequential Intramolecular Interactions that Progressively Block Rb Functions as Cells Move through G1. *Cell* 1999;98(6):859–869. Available at: http://doi.org/10.1016/S0092-8674(00)81519-6
54. Chung JH, Bunz F. Cdk2 Is Required for p53-Independent G2/M Checkpoint Control. *PLoS Genet* 2010;6(2):e1000863. Available at: http://doi.org/10.1371/journal.pgen.1000863
55. Shao H, Cheng HY, Cook RG, Tweardy DJ. Identification and characterization of signal transducer and activator of transcription 3 recruitment sites within the epidermal growth factor receptor. *Cancer Res* 2003;63(14):3923–3930. Available at: http://doi.org/10.1371/journal.pgen.1000863